

Compact Cryogenic Source of Periodic Hydrogen and Argon Droplet Beams for Intense Laser-Plasma Generation

R. A. Costa Fraga,¹ A. Kalinin,¹ M. Kühnel,¹ D. C. Hochhaus,^{2,3} A. Schottelius,¹ J. Polz,⁴ M. C. Kaluza,^{4,5} P. Neumayer,^{2,3} and R. E. Grisenti^{1,6,a)}

¹⁾ *Institut für Kernphysik, J. W. Goethe-Universität, Max-von-Laue-Str. 1, 60438 Frankfurt am Main, Germany*

²⁾ *ExtreMe Matter Institute EMMI and Research Division, GSI Helmholtzzentrum für Schwerionenforschung, Planckstr. 1, 64291 Darmstadt, Germany*

³⁾ *Frankfurt Institute for Advanced Studies, J. W. Goethe-Universität, Ruth-Moufang-Str. 1, 60438 Frankfurt am Main, Germany*

⁴⁾ *Institut für Optik und Quantenelektronik, Max-Wien-Platz 1, 07743 Jena, Germany*

⁵⁾ *Helmholtz-Institut Jena, Helmholtzweg 4, 07743 Jena, Germany*

⁶⁾ *GSI Helmholtzzentrum für Schwerionenforschung, Planckstr. 1, 64291 Darmstadt, Germany*

(Dated: 3 December 2024)

We present a cryogenic source of periodic streams of micrometer-sized hydrogen (H_2) and argon (Ar) droplets as ideal mass-limited target systems for fundamental intense laser-driven plasma applications. The highly compact design combined with a high temporal and spatial droplet stability makes our injector ideally suited for experiments using state-of-the-art low-repetition rate high-power lasers, in which a precise synchronization between the laser pulses and the droplets is mandatory. We demonstrate this explicitly by irradiating Ar droplets with pulses from a Petawatt laser.

A liquid that is forced through a small orifice into vacuum under laminar flow conditions emerges as a continuous, cylindrical jet, before it eventually spontaneously breaks up into a stream of spherical droplets as a result of Rayleigh induced oscillations¹. Liquid jets deliver a uniquely functional, boundary-free and self-replenishing target beam, and have found widespread applications, e.g., in photoelectron spectroscopy², soft X-ray generation³, and for studies of fast structural phase transformations⁴.

Microscopic liquid jets are also very promising candidates for novel studies on intense laser-driven plasma generation. The interaction of ultrashort laser pulses with solid targets allows producing extreme conditions that are relevant to laboratory-scale particle accelerators⁵ and laboratory astrophysics^{6,7}. Here, the laser energy is initially transferred to the target via the generation of relativistic electrons. However, the usually large dimensions of the employed targets, typically flat thin foils of mm^2 to cm^2 size, allow the hot electrons to spread transversely leading to a significant reduction of the energy density in the target. This has immediate consequences for fundamental applications such as ion acceleration⁸ or the efficient heating of the target material. Recent efforts have provided evidence for very efficient bulk heating with the use of nearly mass-limited targets whose transverse dimensions are comparable to the laser focus^{9,10}, but these experiments still suffer from the major drawback that the target must be replaced after each laser shot. Rayleigh droplet beams are extremely attractive with respect to the above applications because, when the Rayleigh in-

stability is induced by an intentionally applied excitation, the triggered breakup process delivers a perfectly periodic stream of identical, isolated droplets at a rate of up to several MHz, thereby enabling detailed scaling studies under highly reproducible conditions¹¹.

In this letter, we present a concept to produce periodic Rayleigh droplet beams of cryogenic gases such as H_2 and Ar, which for many potential laser-plasma applications represent the most appealing target systems. It has been shown numerically that the use of a pure H_2 target characterized by a higher plasma density would significantly increase the efficiency of the proton acceleration process¹², which would be further enhanced by the small droplet size. Hydrogen is also of central importance as model system for studies of the equation of state under high-density plasma conditions that are expected in the interior of giant planets such as Jupiter⁷. Liquid droplets of heavier rare gases such as Ar, on the other hand, are ideally suited for K-shell X-ray spectroscopy studies of the hot electron energy distribution, relaxation, and heating of the bulk target material⁹.

Despite their scientific relevance, producing cryogenic Rayleigh droplet beams proves challenging. The high vapor pressures of liquid Ar and H_2 result in very efficient evaporative cooling upon vacuum expansion. The expanding filament thus rapidly cools below its normal melting point and freezes well before Rayleigh breakup can take place^{4,13}. The freezing of the jet can be circumvented by expanding the liquid into an atmosphere of the respective gas in order to suppress evaporative cooling, before injecting the resulting droplet stream into vacuum. This scheme has been demonstrated for diverse cryogenic gases^{14–16}, but the droplet sources employed in these studies are characterized by large dimensions and a substantial beam angular spread caused by the inter-

^{a)}grisenti@atom.uni-frankfurt.de

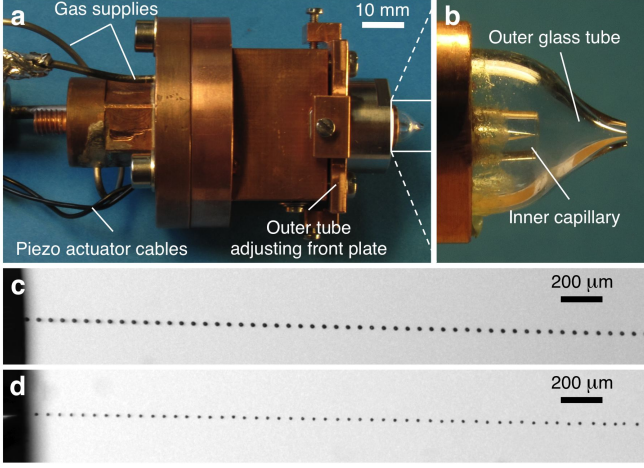


FIG. 1. (a) Picture of the compact cryogenic droplet injector. (b) View of the exit end showing the outer glass tube (exit hole diameter $\approx 140 \div 180 \mu\text{m}$) and the central inner capillary. (c) Stroboscopic image of a periodic Ar droplet beam produced from a $d \approx 10 \mu\text{m}$ diameter capillary orifice at a nominal stagnation source pressure of ≈ 10 bar and at a temperature of ≈ 86 K expanding in Ar gas at a mass flow of ≈ 35 sccm. (d) Periodic H_2 droplet beam produced from a $d \approx 5 \mu\text{m}$ diameter capillary orifice at a nominal stagnation source pressure of ≈ 7 bar and at a temperature of ≈ 14.5 K in H_2 gas at ≈ 70 sccm.

action of the droplets with the co-expanding gas¹⁵. This, in turn, leads to a loss of the spatial synchronization of the triggered droplet beam on the vacuum side, which is of crucial importance when working with low-repetition rate high-power lasers.

Our droplet injector, shown in Fig. 1(a), makes use of a glass capillary that is inserted into an outer glass capillary tube (Fig. 1(b)). As the liquid jet emerges from the inner capillary it expands in an axially co-flowing gas plenum kept at the liquid temperature. The present design enables adjusting the distance between the inner capillary orifice and the outer tube exit hole down to a few millimeters, thus offering a very compact injection source in which the interaction time of the droplets with the co-flowing gas is reduced to a minimum.

The glass capillaries are produced from commercial, pulled Quartz tubes. We break the central neck under the microscope to precisely control the final orifice diameter. Our capillaries are characterized by a sharp orifice edge resulting in ideal conditions for laminar liquid flow. Each capillary is glued into a cylindrical copper plug, which is then sealed by compression onto a custom copper tail-piece. A ring-formed ultrasonic piezoelectric transducer working at frequencies of up to 12.5 MHz is fixed to the capillary holder to generate a periodic disturbance that triggers the breakup of the liquid jet. Precise alignment of the outer glass tube exit aperture with respect to the jet propagation axis is obtained off-line by means of the adjusting front plate (Fig. 1(a)) while producing an isopropanol jet. During cryogenic operation our injector is screwed into the tip end of a continuous helium flow cryo-

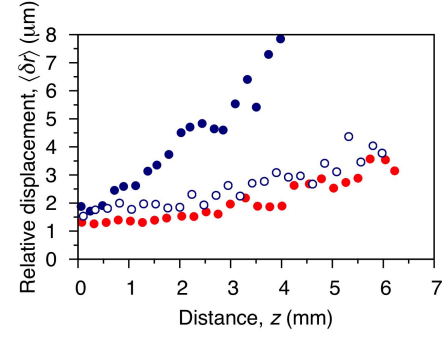


FIG. 2. Relative mean droplet displacement determined from several single-shot stroboscopic images plotted as a function of the distance from the outer tube exit hole. The filled red and blue circles are for Ar and H_2 beams, respectively, expanding in a co-flowing gas. The open symbols are for a H_2 droplet beam produced without external gas atmosphere.

stat for cooling of the source with a temperature stability of better than 0.02 K.

Figures 1(c) and 1(d) show periodic beams of monodisperse Ar and H_2 droplets of diameter $\approx 21 \mu\text{m}$ and $\approx 13 \mu\text{m}$, respectively, jetting from the outer tube exit hole in vacuum. Beam imaging is obtained by using a 4M pixels CCD camera and a long-distance microscope. The function generator driving the piezoelectric actuator also triggers a 10 Hz Nd-YAG laser emitting ≈ 10 ns pulses for stroboscopic backside illumination, as verified by observation of droplets that appear stationary at the piezo driving frequency¹⁷. Stable, satellite-free Ar and H_2 droplet streams are found at excitation frequencies of $f = 0.618$ MHz and 2.1812 MHz, respectively. The Ar and H_2 droplets propagate at a velocity of $v \approx 35 \text{ m s}^{-1}$ and $\approx 131 \text{ m s}^{-1}$, respectively, as inferred directly from the stroboscopic images according to $v = \lambda f$, where λ is the distance between the droplets.

To show that our triggered droplet beams exhibit the necessary spatial stability we compare several single-shot images as those shown in Figs 1(c) and 1(d). The individual frames are used to determine the relative radial (in the image plane) displacements of the center of mass positions of the individual droplets along the stream path¹⁷. The mean relative displacement $\langle \delta r \rangle$ obtained by averaging over all frames is plotted in Fig. 2 as a function of the distance z from the outer tube exit aperture. The increase of $\langle \delta r \rangle$ with increasing z results from the interaction of the droplets with the co-expanding gas prior to vacuum injection, as evidenced by the steeper increase of $\langle \delta r \rangle$ for the H_2 droplets with respect to the much larger Ar droplets. This is further confirmed by the observation of spatially more stable H_2 droplets produced without external gas atmosphere, as shown by the open circles in Fig. 2. Here, the gas that evaporates from the H_2 jet surface is trapped inside the outer glass tube, slowing down the freezing process and thus enabling the triggered jet breakup. However, the droplet stream produced under these conditions is characterized by the occasional ap-

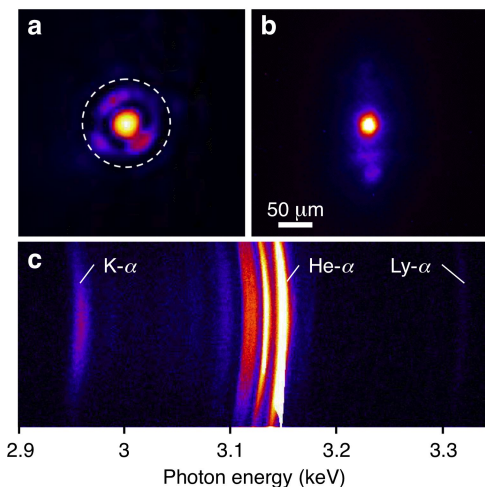


FIG. 3. (a) Focal intensity distribution. The dashed circle indicates the $\approx 21 \mu\text{m}$ diameter Ar droplet. (b) Time-integrated VUV image of the droplet thermal emission. The laser pulse comes from the left. (c) X-ray emission spectra showing the strong Ar K- α and He- α transition lines. The K-shell transitions in intermediate charge state Ar ions are visible as satellites in the spectrum between the K- α and He- α lines.

pearance of solid, several tenths of micrometer long rods formed as a result of short-term jet freezing.

In order to demonstrate the capability of our droplet injector, we performed a proof-of-principle experiment at the PHELIX laser facility¹⁸ by employing Ar droplets as target. Laser pulses from the pre-amplifier stage of ≈ 370 fs duration and containing ≈ 2.5 J energy are focused by a 90° off-axis parabola to a spot of $r_L \approx 3 \mu\text{m}$ radius (see Fig. 3(a)), producing peak intensities of $\approx 10^{19} \text{ W cm}^{-2}$. Temporal synchronization between the droplets and the laser pulses is obtained by triggering the laser amplifier chain with the high-frequency signal that drives the Rayleigh breakup process. The experiments are performed at $z \approx 4 \text{ mm}$, where $\langle \delta r \rangle < r_L$ (Fig. 2), in order to ensure a nearly ideal overlap between the laser beam focus and the Ar droplets. Figure 3(b) shows a time-integrated 2D-image of the VUV emission in a narrow spectral range around 13.7 nm, evidencing a spherical plasma that remains close to the initial droplet size during the thermal emission stage, and thus supporting the conclusion that the droplets are heated isochorically to high-density plasma conditions.

The droplet X-ray emission is spectrally dispersed by a cylindrically curved graphite crystal and is then recorded by a back-illuminated CCD camera. Figure 3(c) shows a typical spectrum that covers the energy range from the Ar cold K- α line at $\approx 2.96 \text{ keV}$ to the Ly- α transition at $\approx 3.32 \text{ keV}$. The estimated conversion efficiency of laser energy into K- α radiation of $\sim 10^{-5}$ is in good agreement with previous experiments employing nearly mass-limited targets^{9,10}, indicating an efficient coupling

of the laser energy to the relativistic electrons.

Whereas a more detailed analysis of the recorded spectra will provide deeper insights into the heating mechanisms of the solid-density Ar droplets, the results presented here clearly demonstrate the potential of our cryogenic droplet beam injection source as a means to deliver ideal mass-limited target samples for fundamental investigations of matter under extreme conditions. In particular, the demonstration of H_2 droplets significantly smaller than in previous studies opens up new possibilities for table-top scale proton accelerators and studies of warm dense matter typical of astrophysical environments.

This work was supported by the Helmholtz Gemeinschaft (Grant No. VH-NG-331) and by the EU within the Seventh Framework Program (Project No. 227431).

- ¹J. Eggers and E. Villermaux, Rep. Prog. Phys. **71**, 036601 (2008).
- ²E. F. Aziz, N. Ottosson, M. Faubel, I. V. Hertel, and B. Winter, Nature **455**, 89 (2008).
- ³L. Malmqvist, L. Rymell, and H. M. Hertz, Appl. Phys. Lett. **68**, 2627 (1996).
- ⁴M. Kühnel, J. M. Fernández, G. Tejada, A. Kalinin, S. Montero, and R. E. Grisenti, Phys. Rev. Lett. **106**, 234501 (2011).
- ⁵J. Fuchs, P. Antici, E. D'Humières, E. Lefebvre, M. Borghesi, E. Brambrink, C. A. Cecchetti, M. Kaluza, V. Malka, M. Manclossi, S. Meyroneinc, P. Mora, J. Schreiber, T. Toncian, H. Pépin, and P. Audebert, Nature Phys. **2**, 48 (2006).
- ⁶S. H. Glenzer and R. Redmer, Rev. Mod. Phys. **81**, 1625 (2009).
- ⁷S. Toleikis, Th. Bornath, T. Döppner, S. Düsterer, R. R. Fäustlin, E. Förster, C. Fortmann, S. H. Glenzer, S. Göde, G. Gregori, R. Irsig, T. Laarmann, H. J. Lee, B. Li, K.-H. Meiwes-Broer, J. Mithen, B. Nagler, A. Przystawik, P. Radcliffe, H. Redlin, R. Redmer, H. Reinholz, G. Röpke, F. Tavella, R. Thiele, J. Tiggesbäumker, I. Uschmann, S. M. Vinko, T. Whitcher, U. Zastra, B. Ziaja, and Th. Tschentscher, J. Phys. B **43**, 194017 (2010).
- ⁸O. Jäckel, J. Polz, S. M. Pfotenhauer, H.-P. Schlenvoigt, H. Schwoerer, and M. C. Kaluza, New Journal of Physics, **12**, 103027 (2010).
- ⁹P. Neumayer, H. J. Lee, D. Offerman, E. Shipton, A. Kemp, A. L. Kritcher, T. Döppner, C. A. Back, and S. H. Glenzer, High Energy Density Phys. **5**, 244 (2009).
- ¹⁰A. Henig, D. Kiefer, M. Geissler, S. G. Rykovanov, R. Ramis, R. Hörlein, J. Osterhoff, Zs. Major, L. Veisz, S. Karsch, F. Krausz, D. Habs, and J. Schreiber, Phys. Rev. Lett. **102**, 095002 (2009).
- ¹¹T. Sokollik, M. Schnürer, S. Steinke, P. V. Nickles, W. Sandner, M. Amin, T. Toncian, O. Willi, and A. A. Andreev, Phys. Rev. Lett. **103**, 135003 (2009).
- ¹²A. P. L. Robinson, P. Gibbon, S. M. Pfotenhauer, O. Jäckel, and J. Polz, Plasma Phys. Control. Fusion **51**, 024001 (2009).
- ¹³B. A. M. Hansson, M. Berglund, O. Hemberg, and H. M. Hertz, J. Appl. Phys. **95**, 4432 (2004).
- ¹⁴M. J. Gouge and P. W. Fisher, Rev. Sci. Instr. **68**, 2158 (1997).
- ¹⁵Ö. Nordhage, Z.-K. Lib, C.-J. Fridén, G. Norman, and U. Wiedner, Nucl. Instr. Meth. A **546**, 391 (2005).
- ¹⁶A. V. Boukharov, M. Büscher, A. S. Gerasimov, V. D. Chernet-sky, P. V. Fedorets, I. N. Maryshev, A. A. Semenov, and A. F. Ginevskii, Phys. Rev. Lett. **100**, 174505 (2008).
- ¹⁷O. Hemberg, B. A. M. Hansson, M. Berglund, and H. M. Hertz, J. Appl. Phys. **88**, 5421 (2000).
- ¹⁸V. Bagnoud, B. Aurand, A. Blazevic, S. Borneis, C. Bruske, B. Ecker, U. Eisenbarth, J. Fils, A. Frank, E. Gaul, S. Goette, C. Haefner, T. Hahn, K. Harres, H.-M. Heuck, D. Hochhaus, D. H. Hoffmann, D. Javorková, H.-J. Kluge, T. Kuehl, S. Kunzer, M. Kreutz, T. Merz-Mantwill, P. Neumayer, E. Onkels, D. Reemts, O. Rosmej, M. Roth, T. Stoehlker, A. Tauschwitz, B. Zielbauer, D. Zimmer, and K. Witte, Appl. Phys. B **100**, 137 (2010).